



ACADÉMIE  
DES SCIENCES  
INSTITUT DE FRANCE

# *Comptes Rendus*

---

## *Chimie*

Vivian Lioret and Richard A. Decréau

**Cherenkov radiation energy transfer from [<sup>18</sup>F]-fluorodeoxyglucose to subphthalocyanine fluorophores**

Volume 27, Special Issue S1 (2024), p. 91-103


Online since: 27 November 2024

Issue date: 24 December 2024

**Part of Special Issue:** French/Nordic Special Issue on Materials and Coordination Chemistry

**Guest editors:** Claude P. Gros (Université de Bourgogne, Dijon, France) and Abhik Ghosh (The Arctic University, UiT, Tromsø, Norway)

<https://doi.org/10.5802/crchim.335>

 This article is licensed under the  
CREATIVE COMMONS ATTRIBUTION 4.0 INTERNATIONAL LICENSE.  
<http://creativecommons.org/licenses/by/4.0/>



*The Comptes Rendus. Chimie are a member of the  
Mersenne Center for open scientific publishing*  
[www.centre-mersenne.org](http://www.centre-mersenne.org) — e-ISSN : 1878-1543



Research article

French/Nordic Special Issue on Materials and Coordination Chemistry

# Cherenkov radiation energy transfer from $[^{18}\text{F}]$ -fluorodeoxyglucose to subphthalocyanine fluorophores

Vivian Lioret<sup>a</sup> and Richard A. Decréau<sup>\*,a</sup>

<sup>a</sup> Université de Bourgogne, Institut de Chimie Moléculaire ICMUB, Sciences Mirande, 21000 Dijon, France

E-mail: Richard.Decreau@u-bourgogne.fr (R. A. Decréau)

**Abstract.** Cherenkov radiation (CR) is an optical light that is emitted during the decay of beta-particle-emitting radionuclides, such as  $^{18}\text{F}$ , which is present in  $[^{18}\text{F}]$ -fluorodeoxyglucose, a well-known tracer used in positron emission tomography. The CR emission occurs from relaxation of molecules of the dielectric medium surrounding the emitted beta-particle. The Cherenkov radiation energy transfer (CRET) to a CR acceptor, such as subphthalocyanine, was analyzed. Subphthalocyanine is a unique concave-shaped  $14\pi$ -electron fluorophore with optical properties. The relevance of such a CR emitter/acceptor couple to performing CRET is discussed.

**Keywords.** Cherenkov radiation energy transfer (CRET), Subphthalocyanine, Cherenkov luminescence imaging (CLI).

**Funding.** CNRS "Chaire d'Excellence", Burgundy/Burgundy Franche-Comté (BFC) Regional Councils (FABER, 3MIM, PARI, respectively), French Ministry of Higher Education, Research and Innovation for a scholarship, ANR-EQPX-IMAPPI, PO-FEDER-FSE Bourgogne, Canceropôle Est (CLI Emergence Project), SATT-SAYENS (CLI-PDT).

**Note.** This proof-of-concept study was performed within the framework of a PhD thesis [1].

*Manuscript received 17 May 2024, revised 26 August 2024, accepted 4 September 2024.*

## 1. Introduction

Cherenkov radiation (CR) is emitted during radionuclide decay when a beta particle is released at a speed that causes the surrounding molecules from the dielectric medium (along the track of the particle) to attain an excited/polarization state. Subsequent relaxation of the surrounding molecules proceeds with light emission, which is called Cherenkov radiation. Overall, such a CR emission occurs when the energy of the beta particle is so high that it can travel even faster than light in a given dielectric medium [2–14]

(which is a medium that could be polarized by an electric field). Hence an analogy can be drawn: the noise emitted when airplanes break the sound barrier may somehow compare with CR, which is emitted when beta particles break the light barrier in a dielectric medium.

The history of CR [2–14] began from its prediction by Oliver Heaviside in 1888, then Arnold Sommerfeld in 1904, and followed by its first observation by Marie Curie who detected its emission from radium samples in the 1910s. Later in the 1920s, Lucien Mallet demonstrated that it was emitted from transparent bodies and could record its spectrum. Then Pavel Cherenkov, a graduate student of Sergei Vavilov at the Lebedev Institute (FIAN), demonstrated its origin

\*Corresponding author

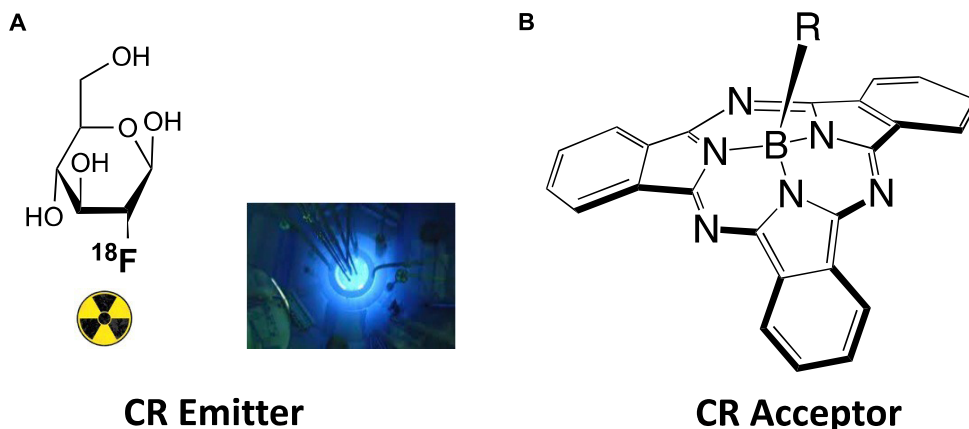


**Figure 1.** (A) CR emitter: [ $^{18}\text{F}$ ]-fluorodeoxyglucose ( $^{18}\text{F}$ -FDG). Inset (left): CR as seen in pools that cool nuclear rods. (B) CR acceptor: subphthalocyanine (**SUB**).

and properties and that it consists of a continuous spectrum. Ilya Frank and Igor Tamm subsequently performed the theoretical interpretation of this emission, and they were awarded the Nobel Prize in 1958 together with Pavel Cherenkov. About 100 years after the first observation of CR, the development of a sensitive camera allowed the use of CR in a variant of optical imaging named Cherenkov luminescence imaging (CLI), first in 2009 in preclinical settings [15–18] and later in 2013 in clinical settings [19,20].

Cherenkov radiation is an alternative light source to perform fluorophore photoactivation, which originates from atomic decay (radionuclides) and surrounding molecules relaxation. Cherenkov radiation energy transfer (CRET) to fluorophores is expected to be efficient as long as there is a good match/overlap between the CR emission spectrum and the fluorophore absorption spectrum [21–27], which roughly falls in the 300–600 nm window of the electromagnetic spectrum. It is required that the optical properties of both the CR emitter and the CR acceptor are acceptable. This means a high CR quantum yield for the former and high brightness B for the latter (with high values of either one or both of its components: fluorescence quantum yield  $\Phi_{\text{F}}$  and molar coefficient absorption  $\epsilon$ ). These matters related to CRET will be addressed on choosing two partners of interest for future biomedical applications, such as  $^{18}\text{F}$  as the CR emitter and subphthalocyanine (**SUB**) as the CR acceptor (Figure 1).

## 2. Results and discussion

### 2.1. Synthesis and radiosynthesis of CR emitter and CR acceptor

#### 2.1.1. CR emitter: fluorine-18 ( $^{18}\text{F}$ ) in [ $^{18}\text{F}$ ]-fluorodeoxyglucose [ $^{18}\text{F}$ ]-FDG

Fluorine-18 ( $^{18}\text{F}$ ) is the most widely used radionuclide for positron emission tomography (PET) imaging in clinical settings [28–31]. Fluorine-18 emits a positron ( $\beta^+$ ) that annihilates on reaction with an electron to produce two gamma rays that are detected and used for PET imaging purposes. The actual study focuses on the ability of the positron to trigger the emission of CR with the surrounding dielectric medium. [ $^{18}\text{F}$ ]-fluorodeoxyglucose ([ $^{18}\text{F}$ ]-FDG) is synthesized by electrophilic or nucleophilic fluorination [28–31] (Figure 2). In electrophilic fluorination, tri-O-acetyl-D-glucal reacted with [ $^{18}\text{F}$ ]- $\text{F}_2$  or [ $^{18}\text{F}$ ]- $\text{CH}_3\text{CO}_2\text{F}$  to produce a mixture of fluorinated molecules. From among these molecules, the difluoroglucose derivative was isolated and subsequently hydrolyzed to form [ $^{18}\text{F}$ ]-FDG (in 8% yield in 2 h). In nucleophilic fluorination, the [ $^{18}\text{F}$ ]- $\text{F}^-$  ion is in the presence of Kryptofix 222<sup>TM</sup>, a cyclic crown ether that binds the potassium ion, which prevents the formation of poorly reactive [ $^{18}\text{F}$ ]-KF and makes [ $^{18}\text{F}$ ]- $\text{F}^-$  more reactive in the nucleophilic substitution. The radioactive anion will displace the triflate leaving group in tetra-O-acetyl-triflate mannose to form [ $^{18}\text{F}$ ]-FDG.

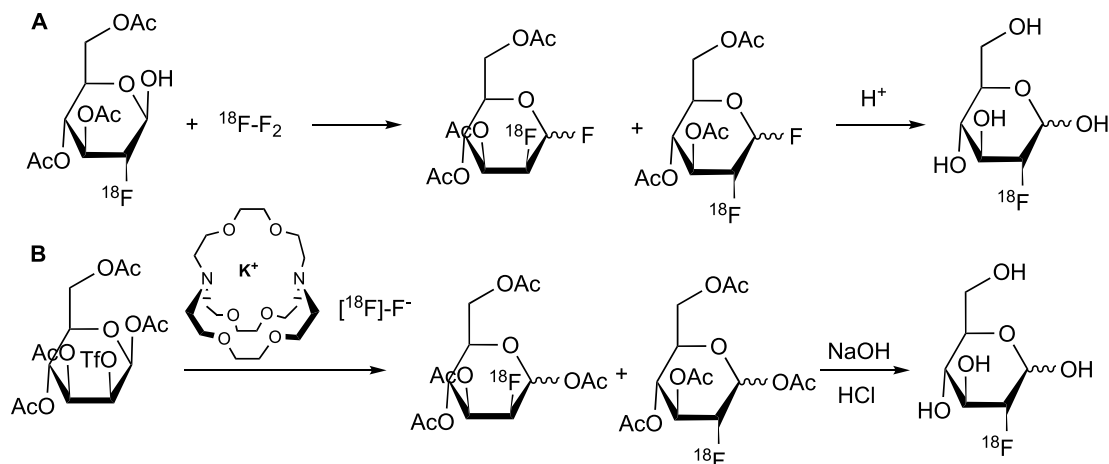


**Figure 2.** [ $^{18}\text{F}$ ]-fluorodeoxyglucose ([ $^{18}\text{F}$ ]-FDG) synthesis, following the electrophilic (A) and nucleophilic (B) fluorination reactions [28–31].

### 2.1.2. CR acceptor: subphthalocyanine

Subphthalocyanines (**SUB**, also reported with the acronym SubPc in the literature) are 14- $\pi$  electron macrocycles that are reported as fluorophores of interest for fluorescence imaging [32,33]. Their shape is unique; they have a domed concave structure, which is an appealing feature in biomedical applications because it does not favor aggregation, a deactivation phenomenon in fluorescence imaging.

The first step in **SUB** platform synthesis (Figure 3) is the dicyanobenzene cyclotrimerization reaction that is typically achieved in 1,2-dichlorobenzene as a solvent under inert atmosphere in the presence of boron trichloride to form golden sparkling chlorosubphthalocyanine dye (SUB-Cl, **1**) of approximately 58% yield. Subsequent reaction of **1** with phenol/hydroxyaryl-containing reagents leads to the replacement of the axial chlorine atom with the corresponding aryloxy substituent of interest, also of 60–64% yield (which corresponds to 35–37% overall yield in **2** and **3**). The first rationale of such an addition was to further address the three-dimensional feature of the dye, that is, subsequently preventing aggregation. The second rationale was to conveniently afford a chemical functionality for further derivatization of **SUB** platforms as with nitrophenoxy substituent in SUB-PH **2** (which could be reduced into an amine for further conjugation). The third rationale was to append a UV/blue

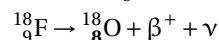
absorbing fluorophore to produce a SUB-COUM **3** dyad, which could undergo more CR absorption and contribute to its transfer toward a less energetic wavelength potentially less absorbed by biological tissues.

## 2.2. Luminescence studies: CR emitter, CR acceptor, and their combination to achieve CRET

### 2.2.1. CR emitter: $^{18}\text{F}$

Theory [31]

- Fluorine-18 ( $^{18}\text{F}$ ) is a “neutron-deficient” or “proton-rich” radionuclide that decays by emitting a positron ( $\beta^+$ ) particle, a neutrino ( $\nu$ ), and its daughter radionuclide  $^{18}\text{O}$  (the atomic number of which is one unit less than that of its starting  $^{18}\text{F}$  parent):



- $^{18}\text{F}$  decay follows the *radioactivity decay law* (Equation (1)):

$$A_t = A_0 e^{-\lambda t} \quad (1)$$

*Parameters of the equation:*  $A_t$ , activity at time  $t$ ;  $A_0$ , activity at  $t = 0$ ;  $\lambda$ , decay constant—it is the probability of disintegration per unit time and it is related to the half-life ( $0.693/t_{1/2}$ );  $t_{1/2}$ , half-life of the

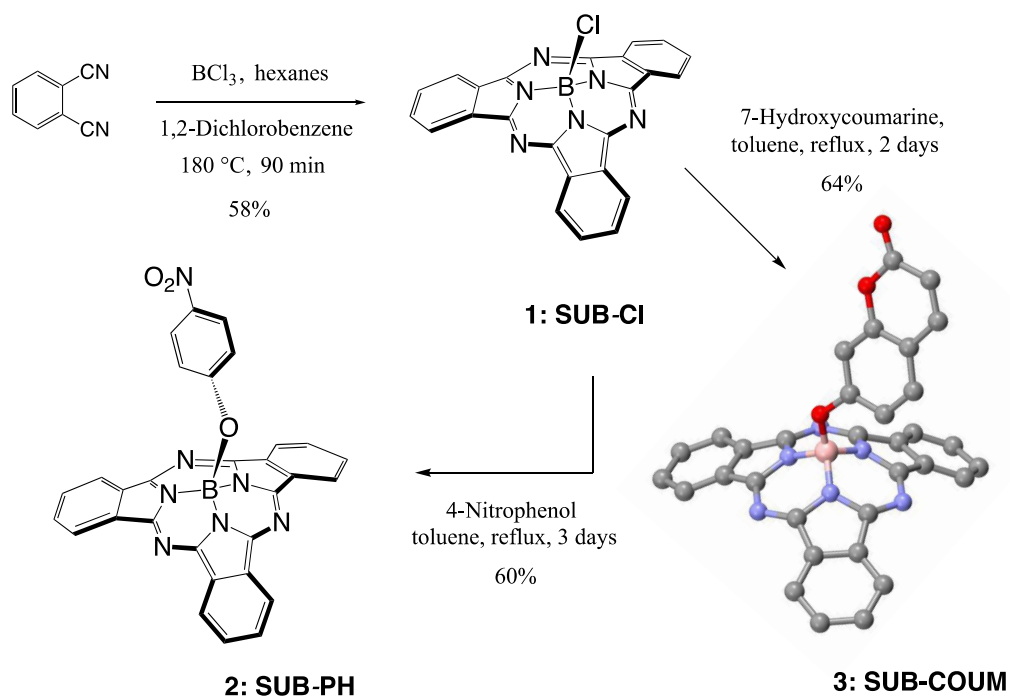


**Figure 3.** Syntheses of subphthalocyanine (SUB) targets bearing three distinct axial features: a chlorine atom (SUB-Cl, 1), a nitrophenoxy group (SUB-PH, 2), and a coumarin (SUB-COUM, 3) [32,33].

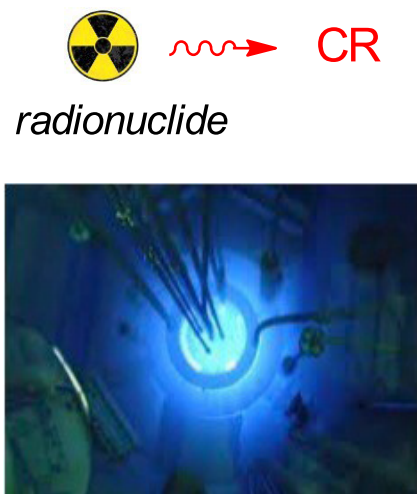


**Figure 4.** Emission of the Cherenkov Radiation (CR) from radionuclides, and as it is seen in pools that cool nuclear rods.

radionuclide, the time the starting activity drops to one half—it is related to activity  $A$

and the number of radioactive atoms  $N$ ; activity of a radionuclide, or radioactivity, is the disintegration rate:  $A = \lambda N = -dN/dt$ .

Equation (1): radioactivity decay law.

- To achieve CR emission (Figure 4), the energy of the beta particle emitted by a radionuclide during the decay process has to be beyond the Cherenkov threshold. Cherenkov emission occurs above this threshold, which is a function of the nature of the medium. When the medium is water, the Cherenkov threshold is 264 keV. The energy of the beta particle emitted by a radionuclide such as fluorine-18 ( $^{18}\text{F}$ ) is 634 keV, which makes it a good candidate for CLI because it is about 2.5-fold beyond the Cherenkov threshold [2–14].
- The number of Cherenkov photons emitted follows the equation reported by Ilya Frank and Igor Tamm (Equation (2)) [2–14]:

$$\frac{dN}{dx} = 2\pi\alpha \left( \frac{1}{\lambda_1} - \frac{1}{\lambda_2} \right) \left( 1 - \frac{1}{\beta^2\eta^2} \right) \quad (2)$$

*Parameters of the equation:*  $dN/dx$ , number of photons per unit of path length whose wavelength is between the  $\lambda_1$  and  $\lambda_2$  intervals;  $\alpha$ , fine structure constant (1/137);  $\beta$ , velocity of the particle (in the medium) divided by that in vacuum (c);  $\eta$ , refractive index (RI).

Equation (2): determination of the number of Cherenkov photons generated during radionuclide decay.

- The number of optical photons (400–800 nm) per nuclear decay is reported to be 0.8–1.4 photons per decay of  $^{18}\text{F}$  atom on a 50  $\mu\text{m}$  step path [15–18]. A Monte Carlo simulation showed that CR emitted from  $^{18}\text{F}$  is confined within 0.3 mm [15–18].
- **CR yield is a function of three parameters:**
  - \* A—energy of the beta particle
  - \* B—activity loaded
  - \* C—RI of the medium

### Experiment

Three parameters governing radiance/CR yield were examined throughout the studies. The emission of CR was recorded both on a spectrofluorometer and on an optical imager.

\* **A—energy of the beta particle.** Experiments were conducted on the spectrofluorometer. The fluorescence cell was filled with a solution of a [ $^{18}\text{F}$ ]-FDG (34.5 MBq) and recording was achieved on a bioluminescence mode (no laser irradiation) with maximum open slits and maximum scans. Under the experimental conditions, a spectrum develops, which is UV/blue weighted (Figure 5). The CR profile is the same from one radionuclide to another. When the energy of the beta particle is raised, such as  $^{90}\text{Y}$  ( $E_\beta = 2.2$  MeV), the luminescence intensity is raised compared to  $^{18}\text{F}$  ( $E_\beta = 0.63$  MeV). Hence,  $^{90}\text{Y}$  appears as a more appealing CR emitter than  $^{18}\text{F}$ . However, the latter was chosen because of its ready availability and for cost reasons.

\* **B—activity loaded.** 96-well plates were filled with 5–25 MBq (0.135–0.676 mCi) [ $^{18}\text{F}$ ]-FDG solution and the remainder of the medium with water. CLI luminescence studies were performed on the *optical imager*, with images recorded just a few minutes after sample deposition, using an open filter mode.

Photon emission is a function of activity: a rise in activity (with no change in medium composition) subsequently leads to a corresponding rise in radiance. The radiance of several activities has been measured by detecting all emitted photons (no filter used) for 1 s (Figure 6).

\* **C—RI of the medium.** The value of the measured radiance varied depending on the nature of the co-solvent. The co-solvent with the highest RI led to the highest radiance as expected from Equation (1) (Figure 7). Hence, when DMSO with RI = 1.477 was used as the co-solvent, a radiance was measured that was 1.2–1.5 times as much as that of other co-solvents, the RIs of which were lower, that is, in the 1.3 range. Conversely a striking observation could be made: although the methanol RI value was slightly lower (1.328) than that of serum (1.34), its radiance evolved the other way around. This may possibly be explained because the RI value is the average of values recorded on the whole UV–vis window. Although the RI value of methanol measured at 400 nm is noticeably higher (1.374) (Figure S1) than that measured at 700 nm (1.320), the reported value (1.331) [34] corresponds to the average value of all other measured RIs at various wavelengths. Hence, at 400 nm, which corresponds to a region of the spectrum where CR emission is more intense, the RI value for methanol (1.374) is higher than that of water (1.34).

#### 2.2.2. CR acceptor: **SUB** (fluorescence studies)

The optical properties of subphthalocyanine measured in toluene indicate a maximal absorption at 562 nm and emission at 572 nm (i.e. 10 nm Stokes shift). It was noted that the fluorescence quantum yield  $\Phi_F$  measured in toluene of the subphthalocyanine dropped when the axial chlorine atom was substituted (0.32 for **1**, 0.17 and 0.19 for **2** and **3**, respectively).

#### 2.2.3. CRET studies

**Rationale.** Hence, studies reported in Sections 2.2.1 (Figure 5) and 2.2.2 (Figure 8) indicate that the spectral overlap between the CR acceptor and the CR emitter is optimum (Figure 9A). Hence, subsequent CRET studies on the optical imager could be performed, the concept of which is depicted in Figure 9B,C, and CLI images displayed in Figure 10.

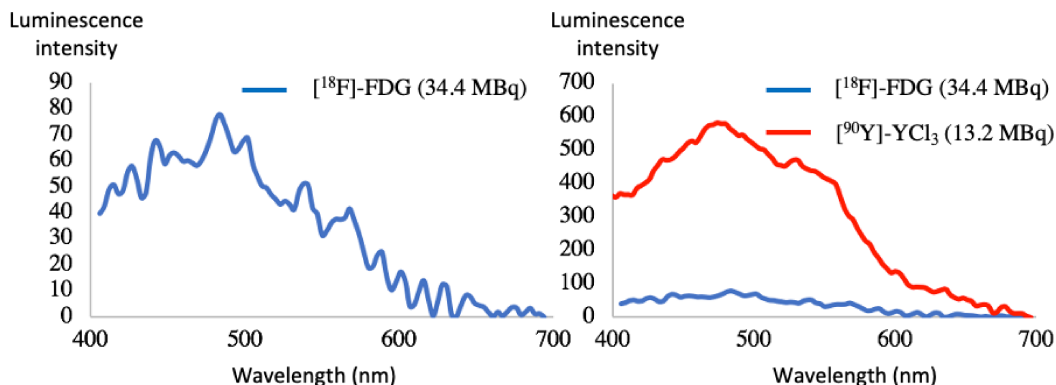


**Figure 5.** Cherenkov radiation emission spectra of [ $^{18}\text{F}$ ]-FDG (34.5 MBq) and [ $^{90}\text{Y}$ ]-YCl<sub>3</sub> (13.2 MBq) [24].

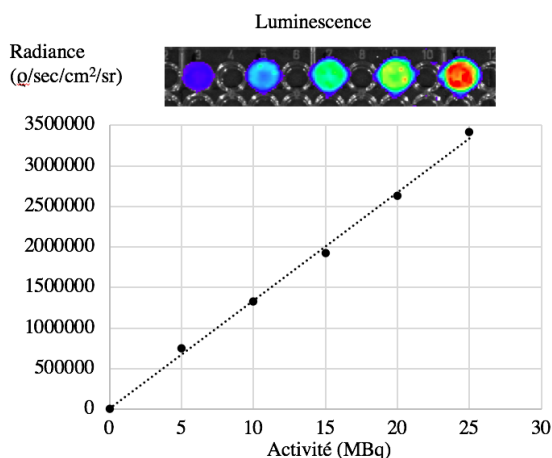


**Figure 6.** Measured radiance as a function of activity in [ $^{18}\text{F}$ ]-FDG [1].

**Experiment.** It was performed in 96-well plates and consisted in mixing a solution of the CR emitter to a solution of the CR acceptor. Hence, a few microliters of a [ $^{18}\text{F}$ ]-FDG solution that corresponds to approximately 10 MBq (0.270 mCi) was added to a solution of 1 mM of subphthalocyanine **SUB-PH 2** or **SUB-COUM 3**. As the radionuclide half-life has to be taken into account at all times ( $^{18}\text{F}$  half-life is 109.8 min) and because the [ $^{18}\text{F}$ ]-FDG provider did not furnish the same volumetric activity (depending on multiple parameters such as the time of delivery and the starting time of the experiment), extreme care had to be taken with the volume added to a well. Hence, adding 10 MBq could vary from 15  $\mu\text{L}$

up to 45  $\mu\text{L}$  depending on the volumetric activity of the stock solution of the purchased radionuclide. To ensure the medium maintains the same composition (and hence the same RI), all controls were diluted the same way.

The first well was filled with [ $^{18}\text{F}$ ]-FDG CR emitter (column 1), the second and third with both CR emitter and subphthalocyanine CR acceptor **SUB-PH 2** (column 2) or **SUB-COUM 3** (column 3), respectively. [ $^{18}\text{F}$ ]-FDG was provided in solution in physiological serum, in which subphthalocyanines **2** and **3** are not soluble. As a result, the latter were dissolved in an organic solvent that could remain miscible with water, such as DMSO. Such a co-solvent was also added to the FDG-containing well to ensure that conditions remain comparable.

**Results.** A first series of radiance measurements were achieved using the  $520 \pm 20 \text{ nm}$  filter. Radiance measured in wells from column 1 that contain *only* CR emitters without **SUB** probes was 1.5-fold higher than that measured in wells from columns 2 and 3 that contain *both* CR emitters and **SUB** probes. This filter overlays a window where the CR spectral emission is significant, which explains why the radiance measured in wells from CR-emitter-only column 1 is high. Conversely, the **SUB** platform absorbs CR in this window as a result of a good spectral overlap of both while **SUB** is not yet detected in such a window. Overall, this explains such a drop in radiance from CR-only wells compared to wells containing CR-absorbing molecules.

Co-solvent used	Refractive index (RI)
Serum <b>(1)</b>	1,34
DMSO <b>(2)</b>	1,4777
CH <sub>3</sub> OH <b>(3)</b>	1,328

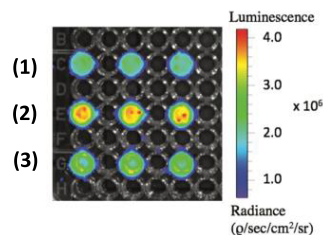


**Figure 7.** Measured radiance of solutions containing [<sup>18</sup>F]-FDG emitter (35 µL solution) and a co-solvent (65 µL) such as serum **(1)**, DMSO **(2)**, and CH<sub>3</sub>OH **(3)** [1]. Radiance values are also reported in a diagram depicted in Figure S2.

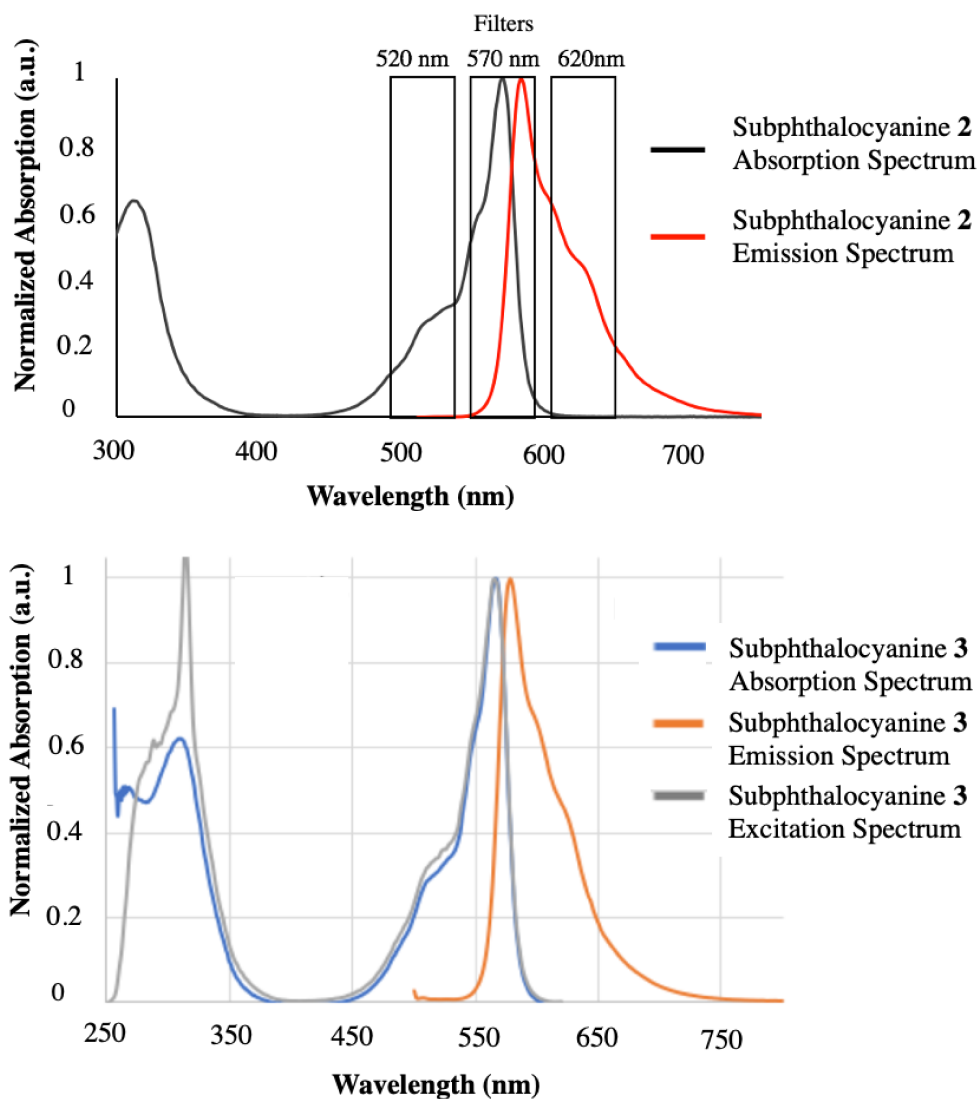


**Figure 8.** Top: Overlay of selected emission filters on the optical imager with subphthalocyanine **SUB-PH 2** absorption spectrum (black) and emission spectrum (red) measured in DMSO/H<sub>2</sub>O 60/40 vol. Bottom: Subphthalocyanine **SUB-COUM 3** spectra: absorption (blue), emission (orange), and excitation (gray) spectra recorded in pure DMSO [1,32,33].



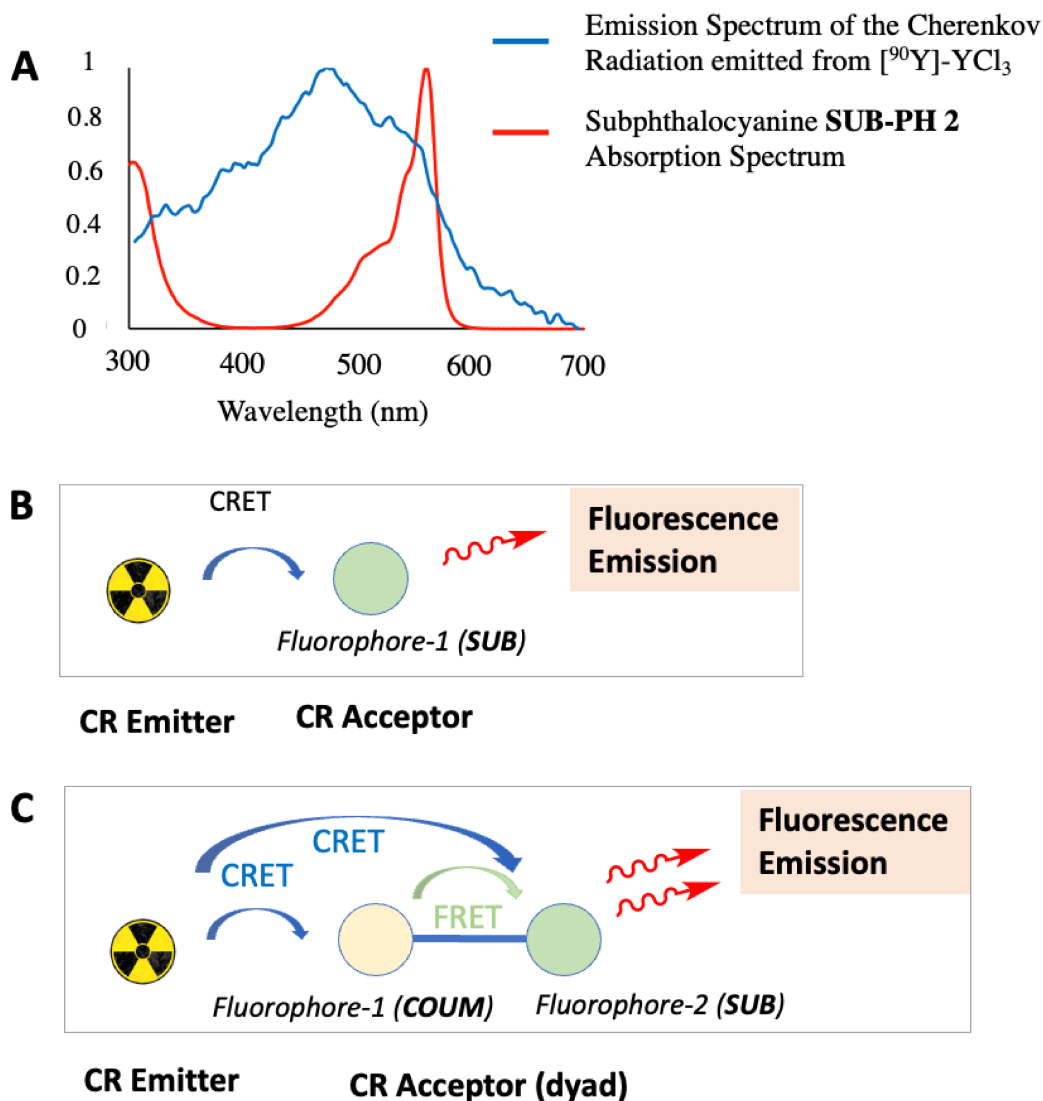


**Figure 9.** (A) Overlay of the Cherenkov radiation emission spectrum from  $[^{90}\text{Y}]\text{-YCl}_3$  (13.2 MBq) (see Figure 5) and the absorption spectrum of subphthalocyanine **SUB-COUM 3** (measured in DMSO) (see Figure 8). (B,C) Depiction of CRET from CR emitter to CR acceptor(s) (fluorophore(s)), subsequently followed by fluorescence emission (from SUB fluorophore only), which is enhanced when COUM antenna is present and undergoes additional CRET transfer and subsequent intramolecular FRET/TBET transfers at the SUB platform (with no expected residual fluorescence emission from COUM, previous studies suggested [1,33]).

A second and third series of radiance measurements were achieved using  $570$  and  $620 \pm 20$  nm filters, respectively. Such windows shift away from the main CR emission peak. As a result, the radiance corresponding to CR emission only (column 1) keeps on dropping from  $570$  to  $620$  nm. Conversely, these filters are overlaid with **SUB** platform emis-

sion spectra, which explains why the radiance is raised in columns 2 and 3, compared to that in column 1 (control). Hence, the most spectacular result shows that the radiance corresponding to subphthalocyanine **SUB-COUM 3** emission is raised by 2.1-fold compared to the radiance to CR-only emitting well. This is because the **SUB** platform is

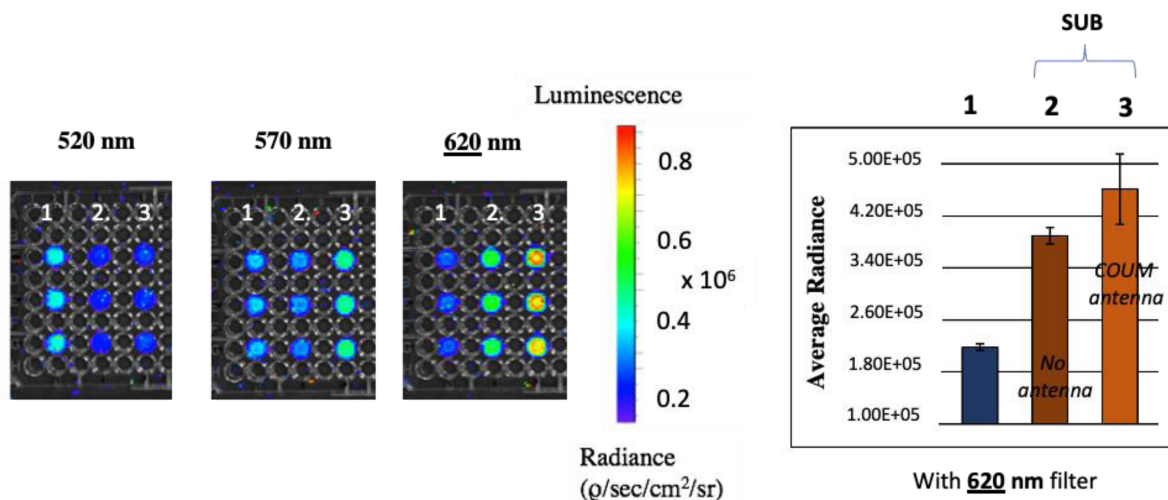


**Figure 10.** Cherenkov luminescence imaging studies: measured radiances of solutions containing [ $^{18}\text{F}$ ]-FDG (10 MBq) CR emitter only (column 1), or CR emitter mixed with subphthalocyanines **SUB-PH 2** (column 2) and **SUB-COUM 3** (column 3). Radiances were measured with filters centered at 520, 570, and 620 nm, respectively.

equipped with a coumarin antenna. Subphthalocyanines not equipped with a **COUM** antenna do not display such a rise in radiance. Earlier results with a non-radioactive light source showed that setting the irradiation at the **COUM** antenna (360 nm) led to an emission corresponding to that of the **SUB** platform and not from that corresponding to **COUM** emission. This suggests a high energy transfer efficiency yield in the form of intramolecular Förster resonance energy transfer (FRET) or through bond energy transfer (TBET) [26,33]. It is first crucial to point out, as mentioned in the previous section, that the fluorescence quantum yields measured for all substituted subphthalocyanines remained comparable. This means that such differences in radiance measured from **SUB-PH 2** to **SUB-COUM 3** is the result of CRET and not from the subphthalocyanine  $\Phi_{\text{F}}$ .

### 3. Conclusion

This proof-of-concept study showed that CR is an alternative light source to photoactivate fluorophore platforms upon CRET, and indicated that the chosen CR emitter/acceptor pair in the actual study ( $^{18}\text{F}/\text{SUB}$ ) was relevant. Regarding the CR emitter ( $^{18}\text{F}$  in [ $^{18}\text{F}$ ]-FDG), despite its potency to emit

CR (0.8–1.4 optical photons (400–800 nm)/decay per 50  $\mu\text{m}$  step size [15–18], also indicated by the energy of its emitted beta particle [ $E_{\beta} = 634$  keV]) that appears to be not as high as that of other radionuclides (up to threefold as less as  $^{90}\text{Y}$ ), it was straightforward to perform its CLI imaging on an optical imager at 10 MBq and to record its emission spectrum on a spectrofluorometer. Moreover,  $^{18}\text{F}$  remains easily accessible and cheap because of its wide availability in the clinical field. Regarding the CR acceptor (**SUB**), despite its brightness (i.e., referring to  $\Phi_{\text{F}}$  and  $\varepsilon$ ) that appears to be not as high as that of other fluorophores (12,500 versus 73,000–88,000 with fluorescein), its absorption spectrum overlaps well with the CR emission spectrum while its unique conical shape makes **SUB** appealing with respect to preventing aggregation and to envisioning future molecular assemblies. Hence, such a **SUB**/ $^{18}\text{F}$  pair enabled achieving CRET and subsequent fluorescence emission from **SUB**. Furthermore, such a proof-of-concept study showed that appending an additional fluorophore onto **SUB** with a good spectral overlap with both **SUB** and CR allowed achieving additional CRET transfers at both **COUM** and **SUB** fluorophores within the dyad together with intramolecular ET transfers (FRET/TBET). This subsequently allowed further rise in radiance toward the targeted

near-infrared (NIR) window. Such an approach is of significant relevance to *in vivo* imaging purposes for two reasons: (a) CR may be considered an alternative to exogenous lasers classically used in fluorophore photoactivation in standard optical imaging, where the radionuclide becomes an embarked (on board) light source, which has advantages with respect to signal-to-background ratios [15–18]; (b) the rationale of the study could be extended to other dyads with much larger pseudo-Stokes-shifts (than that of SUB-COUM 3) in order to achieve fluorescence emission farther in the NIR window where tissues are more transparent. Hence, fluorophores with absorption bands falling within the 300–600 nm window are a good match to CR emission spectrum (albeit residual CR emission is still detected way beyond 600 nm) [21–27]. Moreover, such a study suggests that CRET to other photoactivatable platforms other than fluorophores may potentially be envisioned [21–27].

## 4. Experimental section

### 4.1. Materials and methods

All spectroscopic measurements conducted to thoroughly characterize **SUB** molecules were performed on the PACSMUB (Pôle Chimie Moléculaire) platform at the University of Burgundy.

#### 4.1.1. Nuclear magnetic resonance spectroscopy (NMR)

Measurements were performed on a Bruker at 300 MHz or 500 MHz ( $^1\text{H}$ ), 75 MHz or 125 MHz ( $^{13}\text{C}$ ), and 96 MHz ( $^{11}\text{B}$ ) in  $\text{CDCl}_3$  with the chemical shifts reported as  $\delta$  in ppm relative to TMS (residual chloroform from deuterated chloroform chemical shift was set at 7.26 ppm, and coupling constants expressed in Hz). The following abbreviations were used to describe spin multiplicity: s = singlet, d = doublet, t = triplet, and m = multiplet.

#### 4.1.2. UV-visible spectroscopy

UV-vis measurements were performed on a Shimadzu UV-2550 spectrophotometer in glass cuvettes of  $1 \times 1 \times 3$  cm (1 cm path) and on an Agilent Cary 50 or Cary 60.

#### 4.1.3. Mass spectrometry

(a) Matrix-assisted laser desorption/ionization time of flight mass spectrometry (MALDI-TOF MS): Measurements were performed on Ultraflex II LRF 2000 (Bruker), using dithranol or DHB as a matrix or on a microflex LRF (Bruker). Solutions were prepared by dissolving 1 mg of compound in 1 mL of the appropriate solvent. (b) Electrospray ionization mass spectrometry (ESI MS). Measurements were performed on LTQ Orbitrap XL (Thermo Scientific) coupled to HPLC UltiMate 3000 (Dionex). Solutions were prepared by dissolving 1 mg compound into 1 mL of appropriate solvent and then diluted 100 times with methanol.

#### 4.1.4. High-pressure liquid chromatography separation and analysis (HPLC)

*System A*: HPLC-MS (Hypersil C18 column, 2.6  $\mu\text{m}$ , 2.1  $\times$  50 mm) with  $\text{H}_2\text{O}$  0.1% FA as eluent A and  $\text{CH}_3\text{CN}$  0.1% FA as eluent B (linear gradient from 5 to 100% of B [5 min] and 100% of B [1.5 min]) at a flow rate of 0.5 mL/min. UV detection was achieved at 201, 290, 550, 690, and 750 nm. *System B*: HPLC (Hypersil C18 column, 5  $\mu\text{m}$ , 10  $\times$  250 mm) with  $\text{H}_2\text{O}$  0.1% FA as eluent A and  $\text{CH}_3\text{CN}$  0.1% FA as eluent B (linear gradient from 20 to 60% of B in 40 min) at a flow rate of 3.5 mL/min. UV detection was achieved at 700 and 780 nm.

#### 4.1.5. Fluorescence measurement and quantum yield

Fluorescence measurements were performed on Horiba Jobin Yvon Fluorolog spectrofluorometer (software FluorEssence).

**Cherenkov luminescence imaging studies: CR detection and CRET studies** were performed at the CGFL Preclinical Imaging and Radiotherapy Platform (PIRP). All protocols strictly comply with standards of radioprotection and regulations of the *French Nuclear Safety Authority* (ASN). CLI studies were performed using [ $^{18}\text{F}$ ]-FDG as a source of fluorine-18 radionuclide. [ $^{18}\text{F}$ ]-FDG was provided by Curium (Cyclopharma), and the sample activity was measured upon reception on site. Studies were performed as follows: (a) Agilent Cary Eclipse spectrofluorometer (sensitivity: signal-to-noise measurements of Raman band of water 1/700) in quartz cuvette  $1 \times 1 \times 3$  cm (1 cm path). (b) IVIS Lumina III optical imager using 96-well plate (200  $\mu\text{L}$ ).

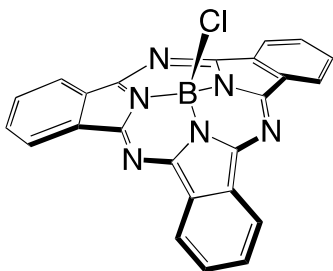
## 4.2. Synthesis and radiosynthesis

[ $^{18}\text{F}$ ]-fluorodeoxyglucose ( $^{18}\text{F}$ -FDG) was purchased from Cyclopharma, which produces it on site in Dijon. Its radiosynthesis was performed on site following a reported method [28–31]. Organic syntheses of subphthalocyanines SUB-Cl, SUB-PH, and SUB-COUM were previously reported [32,33] and optimized as follows.

### 4.2.1. Synthesis of *B-chloro*

#### [*subphthalocyaninato*]boron(III): SUB-Cl 1

A 1 M solution of  $\text{BCl}_3$  in hexane (20 mL, 20 mmol) was slowly added under nitrogen atmosphere to a solution of phthalonitrile (1.06 g, 8.27 mmol) in dry dichlorobenzene (45 mL). Next, hexane was removed on heating the mixture at 70 °C for 30 min. A condenser was subsequently appended to the flask, and heating of the reaction mixture was raised to 180 °C and carried on for 1.5 h. The color of the mixture that was initially light milky yellow turned to dark purple on heating. On cooling, a precipitate formed, which was isolated by filtration. It was subsequently washed with methanol and pentane and then dried under reduced pressure to obtain **SUB-Cl 1** (700 mg, 58%).  $^1\text{H}$  NMR (500 MHz,  $\text{CDCl}_3$ , 300 K, Figure S3):  $\delta$  (ppm) = 7.95 (m, 6H), 8.90 (m, 6H). HR-MS ESI:  $m/z$  431.0966  $[\text{M}+\text{H}]^+$  (calcd for  $\text{C}_{24}\text{H}_{13}\text{BClN}_6^+$ : 431.0978). HP-LC analysis (system A): retention time 5.83 min.

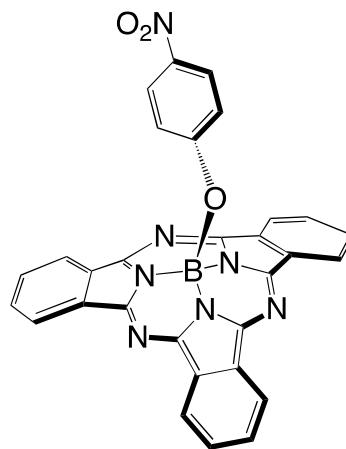


### 4.2.2. Synthesis of *B-(4-nitrophenoxy)*

#### [*subphthalocyaninato*]boron(III): SUB-PH 2

To a solution of **SUB-Cl 1** (50 mg, 0.12 mmol) in toluene (3 mL) was added 4-nitrophenol (81 mg, 0.58 mmol). The reaction mixture was heated under reflux conditions for 3 days and monitored by LCMS. The solvent was removed under reduced pressure. Then the crude product was subjected to a short alumina gel column chromatography (eluent: dichloromethane) to remove the excess of unreacted

phenol, yielding 37 mg (60%) of pure **SUB-PH 2**.  $^1\text{H}$  NMR (300 MHz,  $\text{CDCl}_3$ , 300 K, Figure S4):  $\delta$  (ppm) = 5.37 (d,  $^3J = 9.2$  Hz, 2H), 7.64 (d,  $^3J = 9.2$  Hz, 2H), 7.89 (m, 6H), 8.84 (m, 6H).  $^{13}\text{C}$  NMR (75 MHz,  $\text{CDCl}_3$ , 300 K):  $\delta$  (ppm) = 118.3, 122.1, 125.0, 129.9, 130.7, 141.3, 151.2, 158.5.  $^{11}\text{B}$  NMR (96 MHz,  $\text{CDCl}_3$ , 300 K):  $\delta$  (ppm) = -14.93 (s, 1B). UV-vis (THF),  $\lambda_{\text{max}}$  (nm) ( $\epsilon \times 10^3 \text{ L}\cdot\text{mol}^{-1}\cdot\text{cm}^{-1}$ ) = 304 (56.7), 562 (86.0). HR-MS ESI:  $m/z$  = 533.1414  $[\text{M}-\text{e}]^+$  (calcd for  $\text{C}_{30}\text{H}_{16}\text{BN}_7\text{O}_3^+$ : 533.1402).  $\Phi_{\text{F}}$  (THF) = 0.17 (reference: rhodamine 6G in solution in ethanol).



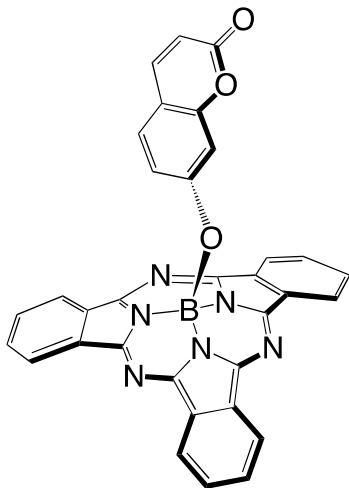
### 4.2.3. Synthesis of *B-(coumarinoxy)*

#### [*subphthalocyaninato*]boron(III):

#### SUB-COUM 3

To a solution of **SUB-Cl 1** (30 mg, 0.07 mmol) in toluene (4 mL) was added 7-hydroxycoumarin (57 mg, 0.35 mmol). The reaction mixture was heated under reflux conditions for 2 days and monitored by LCMS. Thereafter, the solvent was removed under reduced pressure and the crude product was subjected to alumina gel column chromatography using dichloromethane as the eluent to yield 25 mg (64%) of pure **SUB-COUM 3** as a purple solid.  $^1\text{H}$  NMR (500 MHz,  $\text{CDCl}_3$ , 300 K, Figure S5):  $\delta$  (ppm) = 5.27 (d,  $J = 2.2$  Hz, 1H), 5.33 (dd,  $J = 8.5, 2.3$  Hz, 1H), 6.08 (d,  $J = 9.4$  Hz, 1H), 6.83 (d,  $J = 8.4$  Hz, 1H), 7.36 (d,  $J = 9.4$  Hz, 1H), 7.93 (m, 6H), 8.87 (m, 6H).  $^{13}\text{C}$  NMR (125 MHz,  $\text{CDCl}_3$ , 300 K):  $\delta$  (ppm) = 161.25, 156.62, 155.03, 151.61, 143.30, 131.07, 130.22, 128.29, 122.48, 116.31, 113.35, 113.11, 106.41, 77.41, 77.16, 76.91. HR-MS ESI:  $m/z$  557.1527  $[\text{M}+\text{H}]^+$  (calcd for  $\text{C}_{33}\text{H}_{18}\text{BN}_6\text{O}_3^+$ : 557.1528). HP-LC analysis (system A): retention time 5.68 min, 100% MeCN, 0.1% TFA.  $\Phi_{\text{F}}$

(THF) = 0.19 (reference: rhodamine 6G in solution in ethanol).



### 4.3. Luminescence studies

#### 4.3.1. Fluorescence

##### Fluorescence measurement and quantum yield.

Fluorescence measurements were performed on the Horiba Jobin Yvon Fluorolog spectrofluorometer (software FluorEssence) at 25 °C or 37 °C (using a temperature control system combined with water circulation), with standard fluorometer cells (Labbox, LB Q, light path: 10 mm, width: 10 mm, chamber volume: 3.5 mL). Fluorescence quantum yields were calculated using rhodamine 6G in ethanol ( $\Phi_F = 0.96$ ), Nile blue in ethanol ( $\Phi_F = 0.27$ ), and indocyanine green in DMSO ( $\Phi_F = 0.11$ ) as reference. Excitation was performed at 488 nm (rhodamine 6G), 610 nm (Nile blue), or 725 nm (indocyanine green) for both the sample and the reference. Emission spectra were recorded upon excitation (at a given wavelength) at absorbance intensity between 0.02 and 0.09 (a.u.). Fluorescence quantum yields ( $\Phi_F$ ) were determined by the comparison method, using the following equation:

$$\Phi_F = \Phi_F(\text{Std}) \times \left( \frac{\eta}{\eta(\text{Std})} \right)^2 \times \left( \frac{1 - 10^{-\text{Abs}}}{1 - 10^{-\text{Abs}(\text{Std})}} \right) \times \left( \frac{A(\text{Std})}{A} \right)$$

Here, Std corresponds to standard;  $\Phi_F$  and  $\Phi_F(\text{Std})$ , fluorescence quantum yields;  $\eta$  and  $\eta(\text{Std})$ , RIs of solvent;  $A$  and  $A(\text{Std})$ , areas under the fluorescence curves;  $\text{Abs}$  and  $\text{Abs}(\text{Std})$ , absorbances at excitation wavelength (488 nm).

#### 4.3.2. Cherenkov luminescence imaging studies: CR detection and CRET studies

(a) On the Agilent Cary Eclipse spectrofluorometer (measurement parameters: bioluminescence mode, gate time of 10 s, 20 nm emission slit, 3 nm of data interval, Savitzky smoothing factor 5): (i) CR detection: a solution of radioactive species ( $[^{18}\text{F}]\text{-FDG}$  or  $[^{90}\text{Y}]\text{-YCl}_3$ ) was mixed with saline solution (0.9% NaCl) to attain a total volume of 1 mL. (ii) CRET studies (radiofluorescence measurements): 400  $\mu\text{L}$  of fluorophore ( $10^{-3}$  M in a water miscible solvent) was mixed with a solution of radioactive species ( $[^{18}\text{F}]\text{-FDG}$  or  $[^{90}\text{Y}]\text{-YCl}_3$ ), the volume of which was varied because it depends on the desired level of radioactivity to introduce in the cuvette. Subsequent addition of saline solution (0.9% NaCl) was made to attain an overall volume of 1 mL. (b) On the IVIS Lumina II optical imager (measurement parameters: bioluminescence mode, on the open filter mode or with filters, with an acquisition time from 1 s to 1 min). CR detection and CRET studies: The experiment was performed in triplicate on addition of the following solution in each subphthalocyanine-containing well: 10  $\mu\text{L}$  of the subphthalocyanine stock solution (1 mM in DMSO), 32  $\mu\text{L}$   $[^{18}\text{F}]\text{-FDG}$  corresponding to 10 MBq (in solution in physiological serum, the volume of which was varied because it depends on the desired level of radioactivity to introduce in wells), and 58  $\mu\text{L}$  of DMSO to complete the final volume up to 100  $\mu\text{L}$ . To control wells were added 10 MBq  $[^{18}\text{F}]\text{-FDG}$  and 68  $\mu\text{L}$  DMSO.

#### Declaration of interests

The authors do not work for, advise, own shares in, or receive funds from any organization that could benefit from this article, and have declared no affiliations other than their research organizations.

#### Funding

CNRS “Chaire d’Excellence” (RD, 2010–2015) funds allowed to initiate the Cherenkov Luminescence Imaging (CLI) program. The following are also acknowledged: Burgundy/Burgundy Franche-Comté (BFC) Regional Councils (FABER grant (spectrofluorimeter), 3MIM grant (optical imager), PARI Dual Regional/Université de Bourgogne Innovation Grant

(through “Pharmacoimagerie et Agents Théranostiques” project), French Ministry of Higher Education, Research and Innovation for a scholarship (VL)), both ANR-EQPX-IMAPPI and European Union (PO-FEDER-FSE Bourgogne) for their contribution in purchasing radionuclides, Canceropôle Est and SATT-SAYENS for subsequent funding in subsequent development of the Cherenkov Luminescence Imaging (CLI) and Cherenkov Photodynamic Therapy (CLI-PDT) research programs.

## Acknowledgments

The following are acknowledged: PACSMUB platform for access to NMR and Mass spectrometers, Pre-clinical (PIRP) Platform at CGFL for leaving access to their labs.

## Supplementary data

Supporting information for this article is available on the journal’s website under <https://doi.org/10.5802/crchim.335> or from the author.

## References

- [1] V. Lioret, “Synthèse de molécules optimisées pour l’absorption de la radiation Cherenkov : applications à l’imagerie optique et à la thérapie photodynamique”, PhD thesis, Université de Bourgogne Franche Comté, Dijon, 2019.
- [2] O. Heaviside, *The Electrician*, 1888, **22**, 147-148.
- [3] A. Sommerfeld, *Königliche gesellschaft der Wissenschaften zu Göttingen. Mathematisch Physikalische Klasse Nachrichten*, 1904, 363-439.
- [4] E. Curie, *Madam Curie*, Heinemann, London, 1941.
- [5] L. Mallet, *C. R. Acad. Sci. Paris*, 1926, **183**, 274-275.
- [6] L. Mallet, *C. R. Acad. Sci. Paris*, 1928, **187**, 222-223.
- [7] L. Mallet, *C. R. Acad. Sci. Paris*, 1929, **188**, 445-447.
- [8] Le Monde, N. Vichney, “L’effet Cherenkov et la découverte du Docteur Mallet”, 1958, 9, 4287; Ibid “Un chercheur français, le docteur Mallet, affirme avoir découvert en 1926 le phénomène baptisé “effet Cherenkov” 01/11/1958, 16, 4284.
- [9] L. Mallet, *Archives d’Electricité Médicale*, 1928, **Juillet**, 285-289.
- [10] P. A. Cerenkov, *C. R. Dokl. Akad. Nauk SSSR*, 1934, **2**, 451-454.
- [11] P. A. Cerenkov, *Phys. Rev.*, 1937, **52**, 378-379.
- [12] I. M. Franck, I. G. Tamm, *Dokl. Akad. Nauk SSR*, 1937, **14**, 109-114.
- [13] J. V. Jelley, *Br. J. Appl. Phys.*, 1955, **6**, 227-232.
- [14] P. A. Cerenkov, *Science*, 1960, **131**, article no. 3394, 136-142.
- [15] R. Robertson, M. S. Germanos, C. Li, G. S. Mitchell, S. R. Cherry, M. D. Silva, *Phys. Med. Biol.*, 2009, **54**, N355-N365.
- [16] A. Ruggiero, J. P. Holland, J. S. Lewis, J. Grimm, *J. Nucl. Med.*, 2010, **7**, 1123-1130.
- [17] B. J. Beattie, D. L. J. Thorek, C. R. Schmidlein, K. S. Pentlow, J. L. Humm, A. H. Hielscher, *PLoS One*, 2012, **7**, article no. e31402.
- [18] G. S. Mitchell, R. K. Gill, D. L. Boucher, C. Li, S. R. Cherry, *Philos. Trans. R. Soc. A*, 2011, **369**, 4605-4619.
- [19] A. E. Spinelli, M. Ferdeghini, C. Cavedon, E. Zivelonghi, R. Candalrino, A. Fenzi, A. Sbarbati, F. Boschi, *J. Biomed. Opt.*, 2013, **18**, article no. 20502.
- [20] D. L. J. Thorek, C. C. Riedl, J. Grimm, *J. Nucl. Med.*, 2014, **55**, 95-98.
- [21] M. A. Lewis, V. D. Kodibagkar, O. K. Öz, R. P. Mason, *Opt. Lett.*, 2010, **35**, 3889-3891.
- [22] R. S. Dothager, R. J. Goiffon, E. Jackson, S. Harpstrite, D. Piwnica-Worms, *PLoS One*, 2010, **5**, article no. e13300.
- [23] D. L. J. Thorek, A. Ogirala, B. J. Beattie, J. Grimm, *Nat. Med.*, 2013, **19**, 1345-1350.
- [24] Y. Bernhard, B. Collin, R. A. Decréau, *Chem. Commun.*, 2014, **50**, 6711-6713.
- [25] Y. Bernhard, B. Collin, R. A. Decréau, *Sci. Rep.*, 2017, **7**, article no. 45063.
- [26] V. Lioret, P.-S. Bellaye, C. Arnould, B. Collin, R. A. Decréau, *J. Med. Chem.*, 2020, **63**, 9446-9456.
- [27] V. Lioret, P. S. Bellaye, Y. Bernhard, M. Moreau, M. Guillemain, C. Drouet, B. Collin, R. A. Decréau, *Photodiagnosis Photody. Ther.*, 2023, **44**, article no. 103816.
- [28] S. Yu, *Biomed. Imaging Interv. J.*, 2006, **2**, article no. e57.
- [29] J. S. Fowler, T. Ido, *Semin. Nucl. Med.*, 2002, **32**, 6-12.
- [30] K. Hamacher, H. H. Coenen, G. Stocklin, *J. Nucl. Med.*, 1986, **27**, 235-238.
- [31] G. B. Saha, *Fundamental of Nuclear Pharmacy*, 6th ed., Springer, New-York, Heidelberg, Dordrecht, London, 2010.
- [32] Y. Bernhard, P. Winckler, R. Chassagnon, P. Richard, E. Gigot, J.-M. Perrier-Cornet, R. A. Decréau, *Chem. Commun.*, 2014, **50**, 13975-13978.
- [33] V. Lioret, Y. Roussel, R. A. Decréau, *Dyes Pigm.*, 2020, **183**, article no. 108696.
- [34] H. El-Kashef, *Physica B*, 2000, **279**, 295-301.